Journal of Asian Earth Sciences 156 (2018) 256–264

Contents lists available at ScienceDirect

Journal of Asian Earth Sciences

journal homepage: www.elsevier.com/locate/jseaes

Full length article

Greigite formed in early Pleistocene lacustrine sediments from the Heqing Basin, southwest China, and its paleoenvironmental implications

Xiaoke Qiang[a,*], Xinwen Xu[a,b], Hui Zhao[c], Chaofeng Fu[d]

[a] State Key Laboratory of Loess and Quaternary Geology, Institute of Earth Environment, Chinese Academy of Sciences, Xi'an 710061, China
[b] Shaanxi Key Laboratory of Earth Surface System and Environmental Carrying Capacity, Northwest University, Xi'an 710127, China
[c] Department of Geography, Shaanxi Normal University, Xi'an 710062, China
[d] Key Laboratory of Western Mineral Resources and Geological Engineering, Ministry of Education of China & Chang'an University, Xi'an 710054, China

ARTICLE INFO

Keywords:
Lacustrine sediments
Rock magnetism
Greigite formation
Sedimentary environments

ABSTRACT

The ferrimagnetic iron sulfide greigite (Fe_3S_4) occurs widely in sulfidic lacustrine and marine sedimentary environments. Knowledge of its formation and persistence is important for both magnetostratigraphic and paleoenvironmental studies. Although the formation mechanism of greigite has been widely demonstrated, the sedimentary environments associated with greigite formation in lakes, especially on relatively long timescales, are poorly understood. A long and continuous sequence of Pleistocene lacustrine sediments was recovered in the Heqing drill core from southwestern China, which provides an outstanding record of continental climate and environment. Integrated magnetic, geochemical, and paleoclimatic analysis of the lacustrine sequence provides an opportunity to improve our understanding of the environmental controls on greigite formation. Rock magnetic and scanning electron microscope analyses of selected samples from the core reveal that greigite is present in the lower part of the core (part 1, 665.8–372.5 m). Greigite occurs throughout this interval and is the dominant magnetic mineral, irrespective of the climatic state. The magnetic susceptibility (χ) record, which is mainly controlled by the concentration of greigite, matches well with variations in the Indian Summer Monsoon (ISM) index and total organic carbon (TOC) content, with no significant time lag. This indicates that the greigite formed during early diagenesis. In greigite-bearing intervals, with the χ increase, B_c value increase and tends to be stable at about 50 mT. Therefore, we suggest that χ values could estimate the variation of greigite concentration approximately in the Heqing core. Greigite favored more abundant in terrigenous-rich and organic-poor layers associated with weak summer monsoon which are characterized by high χ values, high Fe content, high Rb/Sr ratio and low TOC content. Greigite enhancement can be explained by variations in terrigenous inputs. Our studies demonstrate that, not only the greigite formation, but also its concentration changes could be useful for studying climatic and environmental variability in sulfidic environments.

1. Introduction

Lake sediments provide continuous, high-resolution records of past climatic and environmental changes and, thus, are increasingly important for studies of past global change and regional environmental evolution (Dearing et al., 2006; Fagel et al., 2007; Liu et al., 2012; Oldfield, 2013; Just et al., 2016). Variations in the mineralogy, concentration, and grain size of magnetic minerals in lake sediments are a sensitive indicator of environmental processes within the terrestrial catchment and can also provide information about the depositional environment and post-depositional processes (Ao et al., 2010; Oldfield, 2013; Chang et al., 2014; Fu et al., 2015; Roberts, 2015; Just et al., 2016). However, the origin of magnetic property variations in lake sediments may be complex. An important primary control is the input of detrital iron oxides, which may reflect variations in weathering, erosion, and sediment transport, as well as other processes (Thompson and Morton, 1979; Oldfield et al., 1985; Evans et al., 1997). However, post-depositional alteration can modify or obscure detrital magnetic signals (Reynolds et al., 1999; Robinson and Sahota, 2000; Roberts and Weaver, 2005; Roberts, 2015).

Post-depositional diagenesis in lake sediments is relatively common and well documented (Snowball and Thompson, 1988; Roberts et al., 1996; Nolan et al., 1999; Reynolds et al., 1999; Demorya et al., 2005; Babinszki et al., 2007; Frank et al., 2007; Ron et al., 2007; Ao et al., 2010; Bol'shakov and Dolotov, 2011; Murdock et al., 2013; Roberts, 2015; Just et al., 2016). In iron-reducing sedimentary environments,

* Corresponding author.
E-mail address: qiangxk@loess.llqg.ac.cn (X. Qiang).

https://doi.org/10.1016/j.jseaes.2018.01.033
Received 3 May 2017; Received in revised form 19 January 2018; Accepted 28 January 2018
Available online 31 January 2018

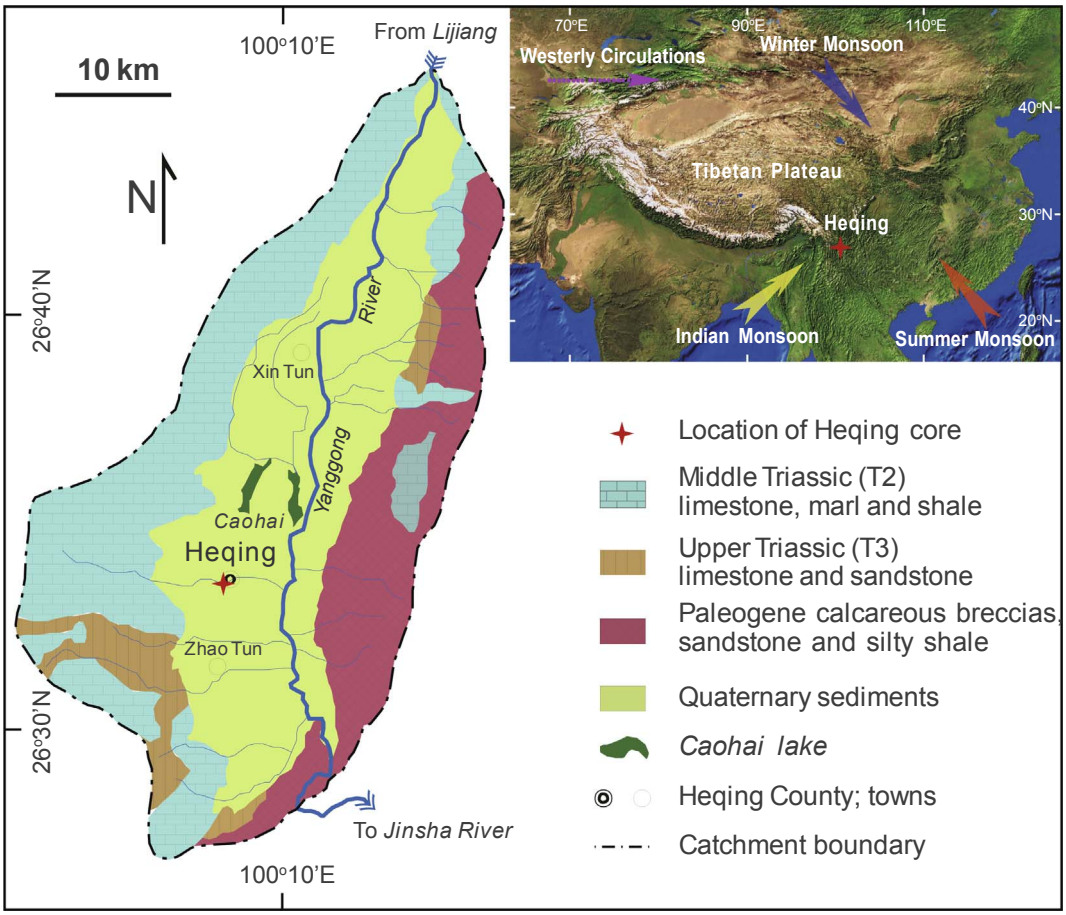

Fig. 1. Location of the study area, wind directions associated with the Asian monsoon systems, and bedrock and surficial geology of the Heqing Basin (An et al., 2011).

microbes utilize iron oxides and dissolve fine-grained detrital ferrimagnetic iron oxide minerals such as magnetite and maghemite. Subsequently, authigenesis of iron sulfides (e.g., greigite) occurs during the process of pyritization (Snowball and Thompson, 1988; Roberts, 1995; Robinson and Sahota, 2000; Kao et al., 2004; Rowan and Roberts, 2006; Chang et al., 2014; Fu et al., 2015; Just et al., 2016).

Greigite (Fe_3S_4) is a widespread ferrimagnetic iron sulfide mineral in sulfidic marine and lacustrine sedimentary environments. During early diagenesis, greigite forms as a precursor to pyrite (FeS_2) in sulfate-reducing environments, and it can also be produced directly by magnetotactic bacteria. Roberts and Weaver (2005) argued that greigite can form at any time during diagenesis if dissolved sulfide and reactive iron are available. Therefore, knowledge of the formation and geological persistence of greigite are important for both magnetostratigraphic and paleoenvironmental studies.

The sulfate content in lakes is much lower than in marine environments and, therefore, sulfate will be exhausted at shallow depths in the sediment or even within the water column. Methanic magnetic mineral diagenesis is thus likely to be more important than sulfidic diagenesis in lake sediments than in marine sediments, although iron sulfide formation is commonplace in lake sediments and thus, sulfidic diagenesis remains important (Roberts, 2015). Overall, the lacustrine sedimentary environments linked to greigite formation, especially in the geological past, are relatively poorly understood. For example, in Lake Qinghai in North China, greigite is present in interglacial sediments with a relatively high total organic carbon (TOC) content (Fu et al., 2015). Conversely, in Lake Ohrid in Macedonia, greigite is present within glacial sediments with a relatively low TOC content (Just et al., 2016).

The Heqing drill core is a long and continuous lacustrine sediment core from Heqing Basin in southwestern China with a basal age of about 2.78 Ma (An et al., 2011 (Supporting Online Material)). Well-characterized climatic cycles, revealed by analysis of environmental proxies indicate that the core provides an exceptional record of continental climate and environment that documents the evolution of the Indian summer monsoon (ISM) (Xiao et al., 2010; An et al., 2011). The lower part of the core contains grayish-green-colored clay sediments, that are indicative of ferruginous and sulfidic diagenetic environments, and within which greigite is present. The aim of the present study is to determine the climatic and environmental control for the greigite formation and greigite concentration changes in these lacustrine sediments.

2. Study area

Heqing Basin (26°27′–26°46′N, 100°08′–100°17′E) is a fault-bounded basin in northwestern Yunnan Province, southwestern China (Fig. 1), situated at the southeastern margin of the Tibetan Plateau, at the terminus of the Hengduan Mountains. It is a closed basin surrounded by mountains with altitudes up to 2500 m. The basin has an N-S orientation and is 22 km in length. The width in the E-W direction is 5–10 km, and the basin area is 144 km^2. The basin receives drainage from the surrounding rivers and streams, and Caohai Lake is located in the current center of the basin. The Yanggong River, which originates in the Yulong Mountains, flows across the basin from north to south and then flows eastward into the Jinsha River. The catchment bedrock consists of Triassic limestone in the west, and Paleogene calcareous conglomerate, sandstone, and silty shale, in the east.

The Heqing drill core (26°33′43.1″N, 100°10′14.2″E, 2190 m) was obtained in 2002 from the center of Heqing Basin. The calibrated depth

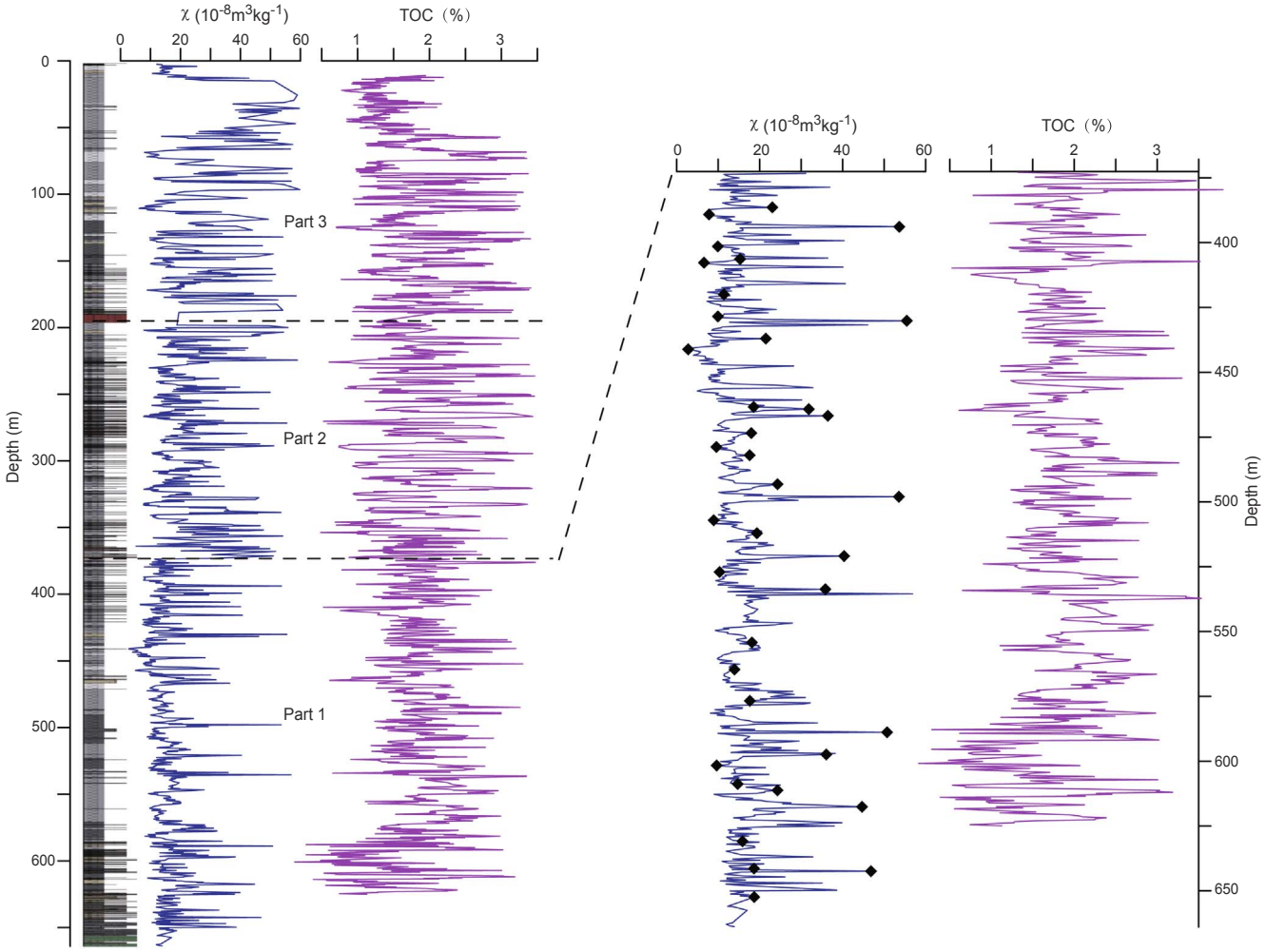

Fig. 2. Variations in lithology, magnetic susceptibility (χ) and TOC content of lacustrine sediments from the Heqing drill core. Diamonds indicate representative samples selected from the peaks and troughs of χ and TOC in P1 for detailed rock magnetic measurements. The boundaries between parts 1, 2, and 3 of the studied core are indicated (see text for explanation).

of the base of the core is 665.8 m and the recovery rate was higher than 97%. The calibrated depth was calculated from the initial drilling depth (737.72 m) after considering depth errors caused by sediment expansion within several cores, the depth of each run, and the drilling deviation in the lower portion of the core (An et al., 2011 (Supporting Online Material)). Except for some 18 m of conglomerate at the base, and two sand layers with fine gravels (372.5–371.9 m and 195.5–189.5 m), the lithology consists mainly of laminated grayish-green calcareous clay and silty clay with thin-bedded silt and fine sand layers (Fig. 2). The core can be divided into three intervals based on tectonic/climatic-sedimentary cycles. In each cycle, the lithology changes from gravel or clay-sand with gravel at the base to silty clay and clay. Part 1 (665.8–372.5 m) consists of dark grayish-green calcareous clays and silty clays with thin silt and fine sand layers; Part 2 (372.5–195.5 m) consists of grayish-green calcareous clays and silty clays with clear bedding, intercalated with light gray silt and fine sand layers; and Part 3 (195.5–0 m) consists of grayish-green and grayish-yellow calcareous clays and silty clays with clear bedding.

3. Sampling and methods

Previous measurements of TOC content and low-field magnetic susceptibility (χ) provided a guide for sample selection in the present study. As illustrated in Fig. 2, high χ values always coincide with low TOC in Part 1 (P1) of the core. A sub-set of 41 representative samples were selected from peaks and troughs of χ in P1 for detailed study.

χ was measured using a Bartington Instruments MS2 magnetic susceptibility meter at a frequency of 465 Hz. Each sample was measured twice and the measurements were averaged. Magnetic susceptibility-versus-temperature curves (χ-T) were measured using a MFK1-FA Kappabridge system with a CS-3 high-temperature furnace. The temperature range was 40–700 °C with a heating rate of 11 °C per minute. The samples were heated and cooled in an argon atmosphere to minimize oxidation of sedimentary components. Low-temperature measurements were made using a MFK1-FA Kappabridge with a CS-L low-temperature furnace. The minimum temperature used was −194 °C. A saturation isothermal remanent magnetization (SIRM) was imparted in a 1 T field before and after thermal demagnetization (as described by Torii et al. (1996)) using a 2-G Enterprises superconducting rock magnetometer (755R). Hysteresis parameters and FORC diagrams were measured using a Model 3900 vibrating sample magnetometer (VSM), to a maximum applied field of 1 T. All measurements were made at the Environmental Magnetism Laboratory in the Institute of Earth Environment, Chinese Academy of Sciences (Xi'an, China). Scanning Electron Microscope (SEM) analyses were made at Northwest University (Xi'an, China) using a Quanta 400 FEG device.

4. Results

4.1. FORC diagrams and hysteresis properties

FORC diagrams are useful for identifying magnetic minerals, their

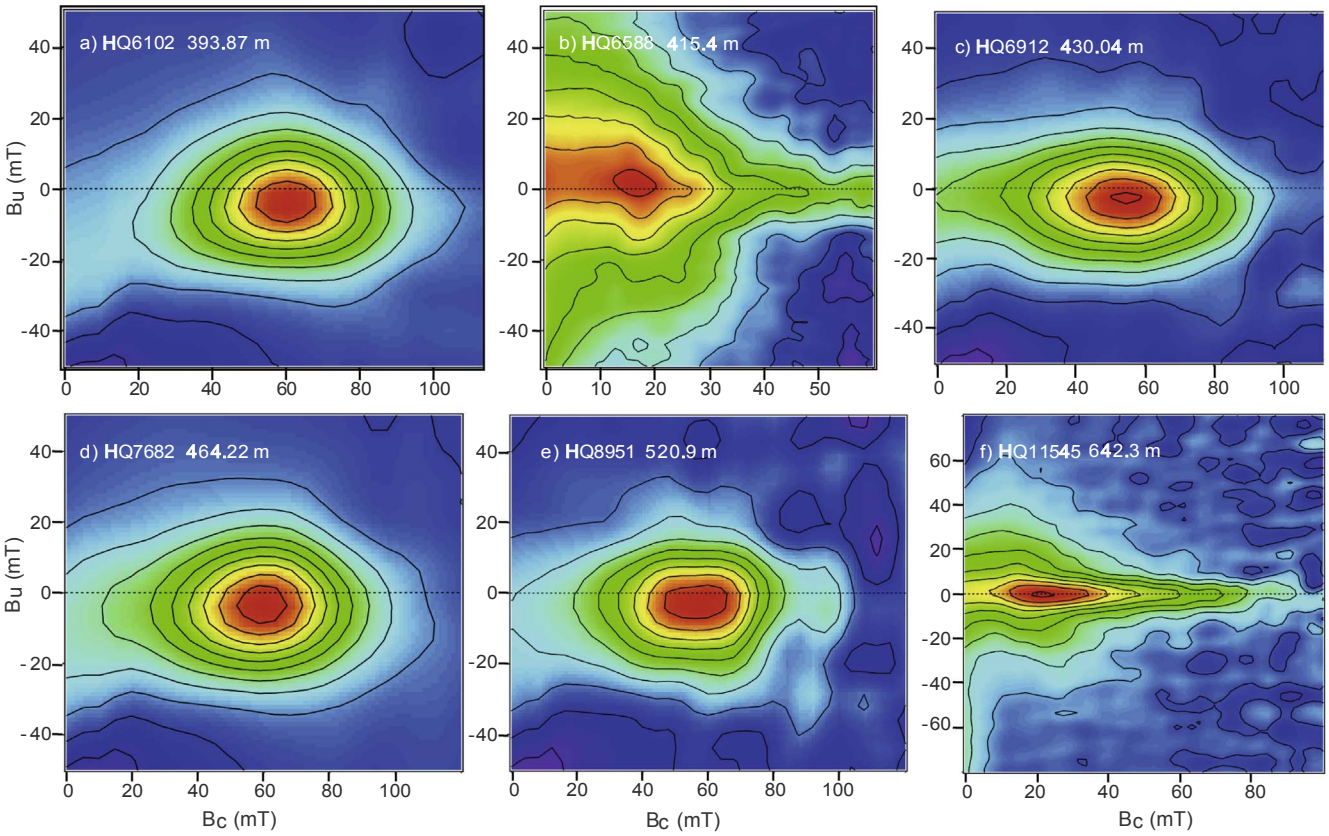

Fig. 3. FORC diagrams for representative samples in P1 from the Heqing drill core. FORC diagrams for samples a, c, and d have concentric contours and a large vertical spread that are indicative of a significant SD contribution. FORC diagrams for samples b and f exhibit PSD behavior.

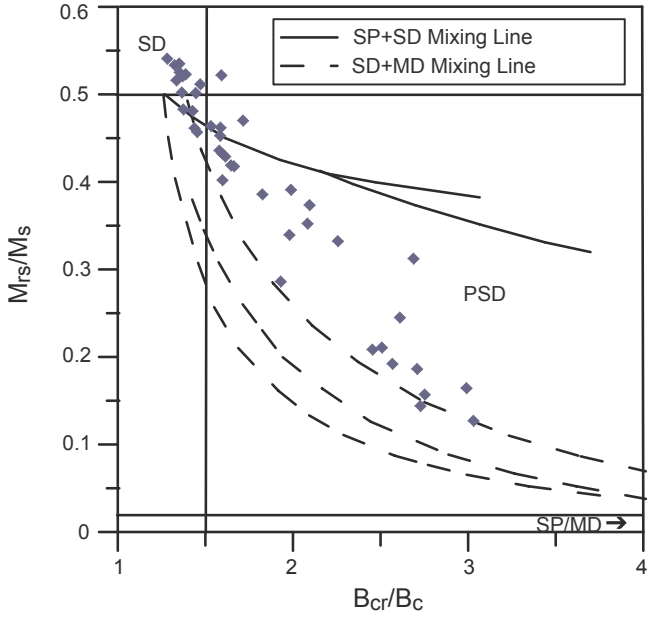

Fig. 4. Hysteresis ratios plotted on a Day plot (Day et al., 1977; Dunlop, 2002) for representative samples from P1 of the Heqing drill core. SD – single domain; PSD – pseudo-single domain; MD – multidomain; SP – superparamagnetic.

domain state, and the presence or absence of magnetostatic interactions in sediment samples (Pike et al., 1999; Muxworthy and Dunlop, 2002; Roberts et al., 2000, 2006, 2014). The studied samples have two different types of FORC diagram. Most samples exhibit single domain (SD) behavior (Fig. 3a, c, d, e), with concentric contours with a large vertical spread that indicates a SD contribution with strong magnetostatic interactions (Pike et al., 1999; Roberts et al., 2000). At the peak of the distribution, H_c is ~59 mT which is typical of SD greigite (Roberts et al., 2000, 2006, 2011; Rowan and Roberts, 2006; Rowan et al., 2009; Chang et al., 2014). A small number of samples have pseudo-single domain (PSD) behavior (Fig. 3b and f). In this case, the diverging contours that extend beyond 30 mT and lack symmetry are indicative of a PSD distribution (Roberts et al., 2000, 2014; Muxworthy and Dunlop, 2002). To confirm the presence of greigite, further rock magnetic analyses and SEM observations were conducted on samples selected on the basis of their FORC diagrams.

The ratio of saturation remanent magnetization to saturation magnetization (M_{rs}/M_s) is plotted against the ratio of coercivity of remanence to coercive force (B_{cr}/B_c) in Fig. 4 (a 'Day plot' – Day et al., 1977; Dunlop, 2002). Samples from P1 are distributed within the SD region and below the SD and superparamagnetic (SP) admixture line in the PSD region (Dunlop, 2002).

4.2. Temperature-dependent magnetic susceptibility (χ)

Temperature-dependent χ is highly sensitive to mineralogical changes during thermal treatment, and such changes can provide information about magnetic mineral composition and magnetic grain-size. The temperature-dependent χ of typical samples from P1 is illustrated in Fig. 5. A major decrease in χ occurs at about 585 °C, which corresponds to the Curie point of magnetite. During heating, there is a sharp χ increase between 400 and 500 °C. This is commonly observed in sediments from reducing environments (Roberts, 1995; Reynolds et al., 1999; Dekkers et al., 2000; Chang et al., 2008; Roberts et al., 2011) and results from pyrite oxidation (Passier et al., 2001; Minyuk et al., 2013; Chang et al., 2014) or the thermal decomposition of greigite (Su et al., 2013; Fu et al., 2015). The pronounced peak at about 510 °C may result from either a Hopkinson peak and/or the neoformation of ferrimagnetic

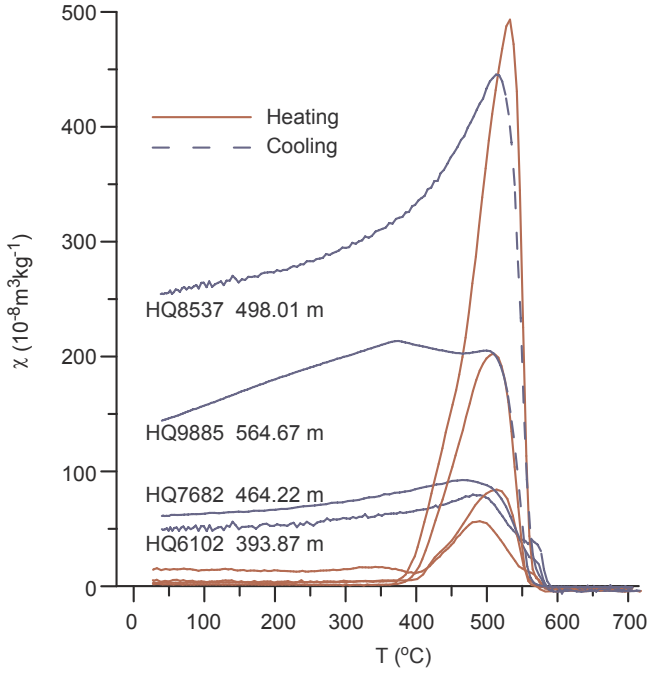

Fig. 5. χ-T curves for representative greigite-bearing samples from P1 of the Heqing drill core. Solid (dashed) lines represent heating (cooling) curves.

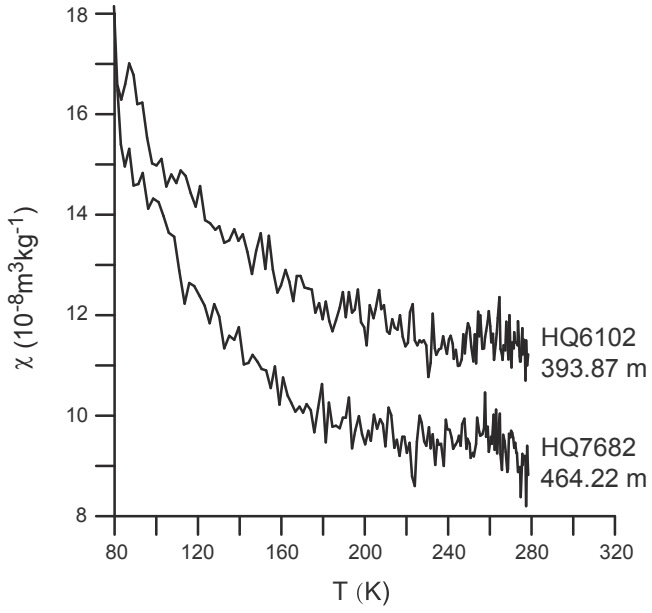

Fig. 6. Low-temperature variation of χ for representative greigite bearing-samples from P1 of the Heqing drill core.

minerals during heating (Deng et al., 2004).

Below room temperature, chemical reactions are suppressed and the magnetic mineral constituents of rocks and sediments do not undergo the alterations that are common at elevated temperatures (Verosub and Roberts, 1995). The χ curves are noisy and do not undergo any noticeable low-temperature variation, such as the Verwey transition in coarse-grained (PSD/MD) magnetite (Fig. 6). This indicates that the sediments have no significant magnetite content because it would have dissolved completely during diagenesis.

4.3. Variation of SIRM imparted before and after thermal demagnetization

The variation of SIRM imparted before and after thermal demagnetization is useful for detecting the presence of greigite (Torii et al., 1996; Sagnotti and Winkler, 1999). The method consists of imparting and measuring an SIRM before and after each thermal demagnetization step. As illustrated in Fig. 7, an SIRM imparted after thermal demagnetization undergoes a distinct decrease above about 225 °C, which indicates the presence of greigite (Roberts, 1995; Torii et al., 1996; Dekkers et al., 2000; Chang et al., 2008; Roberts et al., 2011). In greigite-bearing rocks, the magnetization starts to decrease above 200 °C due to thermal alteration (Roberts, 1995; Dekkers et al., 2000; Roberts et al., 2011). The possibility of maghemite can be excluded because there is no decrease in the corresponding χ-T curve between 300 and 400 °C. Consequently, we conclude that the ferrimagnetic component of samples from P1 of the core is dominated by greigite.

4.4. Results of SEM analysis

The crystal habits and microtextures of greigite-bearing samples in P1 were investigated using SEM (Fig. 8). The magnetic extracts were obtained following the method of Hounslow and Maher (1996). Both bulk samples and magnetic extracts were analyzed. SEM images for greigite were discriminated by Fe and S peaks in energy dispersive spectrometer (EDS) analysis. The greigite grains are clustered among silicate grains, and have perfect octahedral crystal morphology (Reynolds et al., 1999; Roberts and Weaver, 2005; Chang et al., 2008, 2014; Hüsing et al., 2009). Almost every monocrystal has four-sided outlines indicative of sections cut through octahedra (Skinner et al., 1964).

5. Discussion

SIRMs imparted before and after thermal demagnetization (Fig. 7) indicate the presence of greigite (Torii et al., 1996) in P1. The absence of the Verwey transition (indicative of magnetite), the SD distribution, and the peak value of ~59 mT in the corresponding FORC diagram, confirm the presence of authigenic greigite (Roberts et al., 2000, 2006, 2011). Moreover, the SEM image in Fig. 8 reveals the presence of octahedral greigite grains in samples from P1 (Skinner et al., 1964; Reynolds et al., 1999; Chang et al., 2008, 2014; Hüsing et al., 2009; Dong et al., 2013). Further evidence for greigite is shown in Fig. 9, which reveals high M_{rs}/χ values (close to or exceeding 40 kAm^{-1}), high B_{cr} values (~55 mT), and mean values of M_{rs}/M_s and B_{cr}/B_c close to 0.5 and 1.5, respectively (Snowball and Thompson, 1988; Roberts, 1995; Roberts et al., 2011; Reinholdsson et al., 2013; Chang et al., 2014; Kars and Kodama, 2015).

5.1. Early and late diagenesis

As a precursor to pyrite, greigite forms during early diagenesis, and such greigite would give rise to a paleomagnetic signal that is equivalent to that acquired by detrital particles (Tric et al., 1991; Roberts and Weaver, 2005; Chang et al., 2014; Roberts, 2015). On the other hand, there is also substantial evidence of remagnetization resulting from later diagenetic greigite formation (Jiang et al., 2001; Roberts and Weaver, 2005; Rowan and Roberts, 2006; Porreca et al., 2009). Therefore, determining the formation time of greigite is important for both paleomagnetic and paleoenvironmental studies. Greigite is the major magnetic mineral in P1 of the Heqing core, as indicated by the various lines of evidence described above. In greigite-bearing sediments, iron oxide dissolution is expected and in this context the SD grain distributions in Day plots and FORC diagrams are expected to be controlled by the concentration of greigite. The χ variations match well with those of the ISM index and TOC, with no significant time lag (Fig. 9). This indicates that the greigite formation was controlled by variations in the lacustrine and sedimentary environment, which was driven by regional climate change. If the greigite had formed during

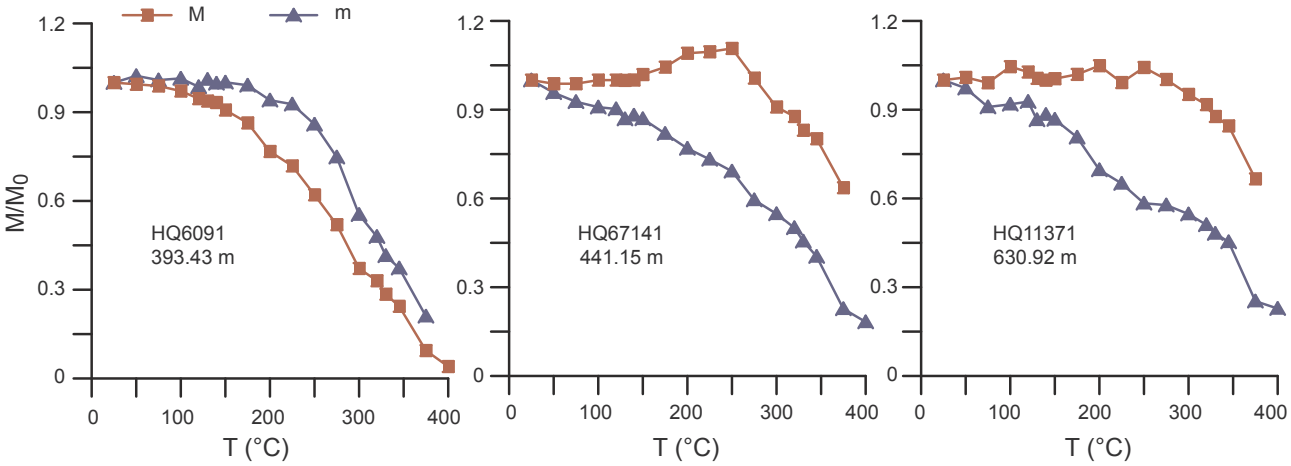

Fig. 7. Variation of normalized SIRM imparted before (blue curve) and after (red curve) thermal demagnetization for representative greigite-bearing samples from P1 of the Heqing drill core. (For interpretation of the references to colour in this figure legend, the reader is referred to the web version of this article.)

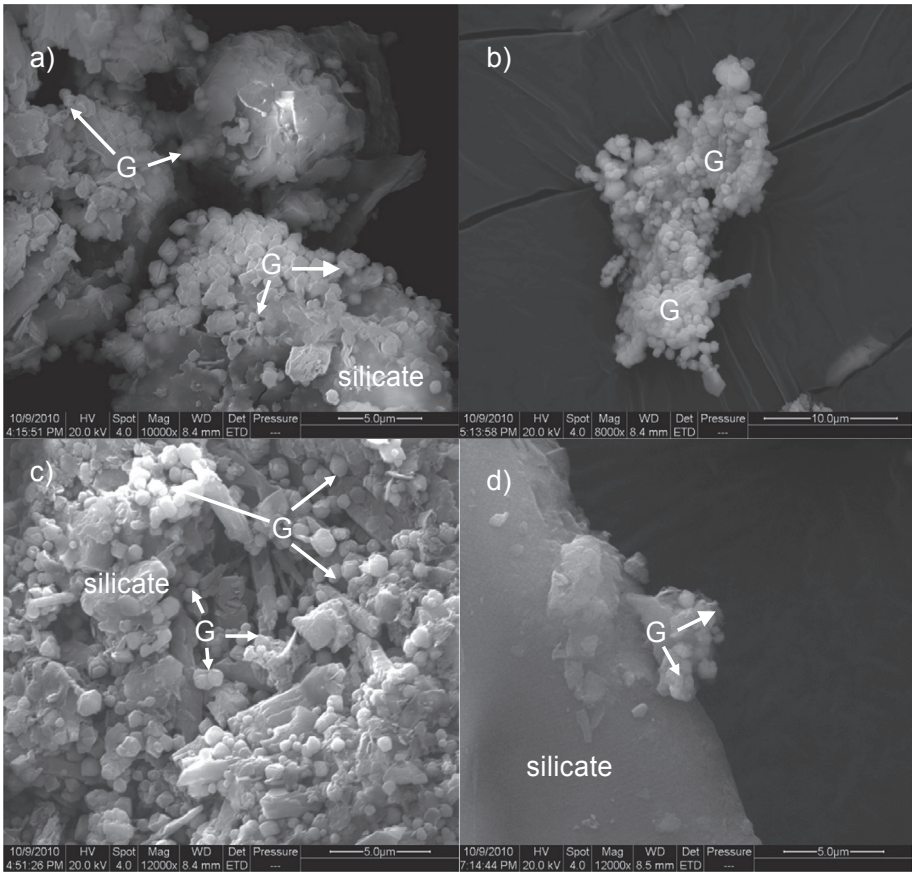

Fig. 8. SEM images of magnetic extracts (a–c) and a bulk sediment sample (d) for representative greigite-bearing samples from P1 of the Heqing drill core. 'G' indicates greigite. SEM images for greigite are identified by Fe and S peaks in energy dispersive spectrometer (EDS) analysis.

late diagenesis, the correlation between χ and the ISM index would not be expected. Thus, we conclude that the greigite in P1 of the Heqing core formed during early diagenesis and that consequently the age model based on magnetostratigraphy is reliable (An et al., 2011).

5.2. Environmental and climatic control of greigite formation in the Heqing core

Combined lithological observations and rock magnetic and geochemical measurements have been used to investigate the potential environmental controls on greigite formation within P1 of the Heqing core. Rock magnetic properties indicate that the greigite in P1 is mainly SD, with high B_c values (often > 30 mT), high M_{rs}/M_s ratios (> 0.4) and low B_{cr}/B_c ratios (< 1.7), as shown in Fig. 9. Greigite is common in samples under 420 m (~1.86 Ma), irrespective of the climate state (strong or weak summer monsoon). In contrast, greigite is seldom above 420 m. Paleoclimatic and paleoenvironmental records like TOC, Rb/Sr ratios, ISM index exhibit an abrupt change at about 420 m. These would indicate that the paleoclimate and paleoenvironment had changed a lot at about 420 m (1.86 Ma) (Xiao et al., 2010; An et al., 2011). The environmental condition correlating to iron sulfide formation would change (Chang et al., 2014; Roberts, 2015). The upper part

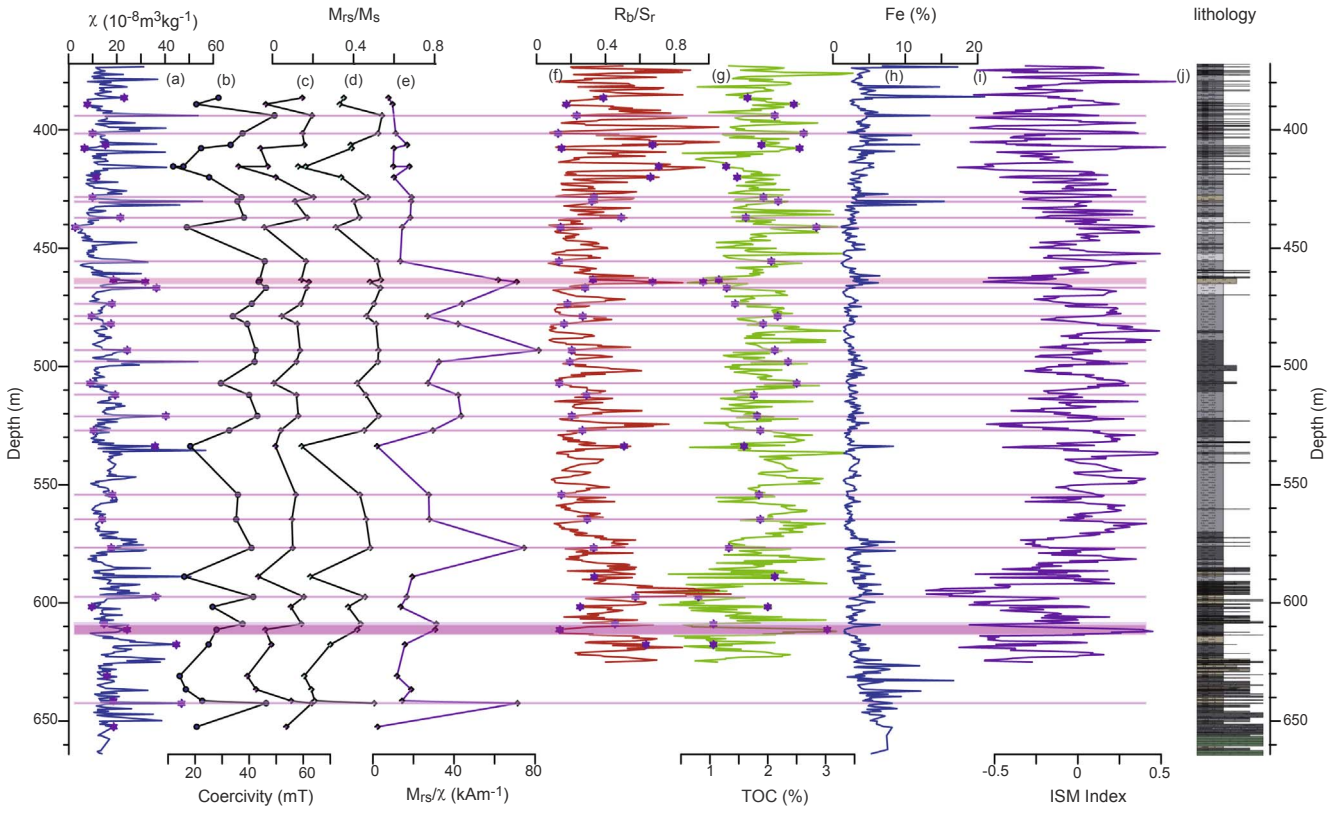

Fig. 9. Magnetic and paleoenvironmental proxies for P1 of the Heqing drill core. (a) Magnetic susceptibility (χ), (b–e) selected rock magnetic properties, (f) Rb/Sr ratio, (g) total organic carbon (TOC) content, (h) Fe content, (i) Indian summer monsoon index (ISM Index), and (j) lithology. The stars in (a), (f), and (g) indicate samples selected for more detailed measurements.

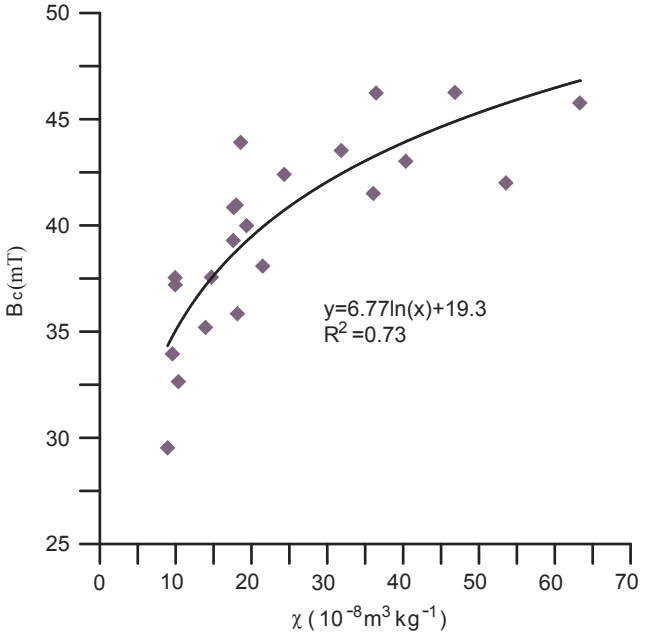

Fig. 10. Relationship between Magnetic susceptibility (χ) and coercivity value (B_c).

should be in favour of pyrite formation, while the lower part prefers greigite formation in sulfidic diagenesis process.

The presence of greigite in sediment is widely used to correlate with climatic and environmental change (Chang et al., 2014; Roberts, 2015). For example, greigite formation is linked to warm/wet climatic period in Lake Qinghai (Fu et al., 2015) and Black Sea (Chang et al., 2014). In contrast, it is correlated to glacial period like Lake Ohrid (Just et al., 2016). However, greigite is common in both strong and weak summer monsoon intervals under 420 m in Heqing core which is different from the case in the Lake Qinghai (Fu et al., 2015) and Lake Ohrid (Just et al., 2016).

χ is a very useful proxy in paleoclimate and paleoenvironment study which dominated by the concentration and grain size distribution of magnetic minerals in sediments (Thompson and Morton, 1979; Evans et al., 1997; Liu et al., 2012). Comparing to magnetite, greigite has a higher B_c value (Roberts et al., 2011; Chang et al., 2014). Therefore, the B_c value of greigite bearing sediments should be dominated by the relative concentration of greigite. As illustrated in Fig. 10, χ and B_c value present a logarithmic relation at a correlation coefficient of 0.73 which indicate that these two parameters was dominated by the same factor, the concentration of greigite. With the χ increase, B_c value increase and tends to be stable at about 50 mT. Althought we can't exclude the effect of different grain size on B_c value of the greigite baering samples. Our rock magnetic tests support the inference that with the concentration of greigite increase, the B_c value of sediments will increase to the B_c value of greigite which mostly suggested from 50 to 60 mT (Rovan and Roberts, 2006; Dunlop, 2002; Roberts et al., 2011). In this context, χ of greigite bearing sediments in P1 of the Heqing core could estimate the greigite concentration variation approximately.

An et al (2011) combined TOC and Rb/Sr records by normalizing each to unit variance, followed by averaging, to produce a stacked Indian summer monsoon (ISM) index. They interpreted the ISM index as indicative of summer monsoon variability, with high values indicating enhanced ISM circulation. Weak summer monsoon intervals of the core, as defined by the ISM Index, have high χ values, high Rb/Sr ratios, low TOC content, and vice versa. Therefore, greigite prefer to be abundant in weak summer monsoon intervals in Heqing core.

Post-depositional degradation of organic matter is a fundamental process for driving early diagenetic chemical change in sedimentary

environments. In sulfidic sediments, iron oxide dissolution (mainly magnetite, maghemite, and hematite) is ubiquitous (Roberts, 2015, and references therein). Dissolved Fe^{2+} released from detrital iron-bearing minerals reacts with dissolved H_2S, which is a by-product of sulfate reduction, to form sedimentary iron sulfides (Berner, 1984). If the rate of Fe^{2+} supply exceeds that of H_2S production, pyritization is retarded or arrested (Kao et al., 2004; Roberts, 2015). In this case, intermediate iron sulfides such as mackinawite and ferrimagnetic greigite can be preserved (Berner, 1984; Kao et al., 2004; Chang et al., 2014; Roberts, 2015). In sulfidic diagenesis environment, greigite concentration should be limited by the relative concentration of dissolved sulfate and reactive iron (Kao et al., 2004; Roberts, 2015).

In P1 of the Heqing core, greigite peaks (high χ value) correlate with high Rb/Sr and low TOC (terrigenous-rich and organic-poor) which similar to that in the Santa Barbara Basin (Blanchet et al., 2009) and the Black Sea (Chang et al., 2014). In lake environments, reactive organic matter is often abundant (Chang et al., 2014) and sulfate content is much lower (Roberts, 2015), in such context, greigite formation appears to have been controlled mainly by terrigenous input (Blanchet et al., 2009). In weak summer monsoon period, enhanced continental weathering (high Rb/Sr ratios) could supply more reactive iron into the paleolake, to prompte greigite formation during the sulfidic diagenesis process.

6. Conclusions

FORC diagrams provide evidence for the presence of greigite throughout the lacustrine sediments of unit P1 of the studied drill core from Heqing Basin. The thermal alteration of magnetic properties between 200 and 400 °C, high B_c values, high M_{rs}/χ ratios, and SEM observations confirm the presence of greigite. Variations in χ correlate with the ISM index and TOC content, with no significant time lag, which indicates that the greigite in the P1 interval of the Heqing core formed during early diagenesis.

Our combined rock magnetic, geochemical, and paleoclimate analyses of the sedimentary sequence from the Heqing Basin enhances our understanding of the environmental and climatic controls on greigite formation in lake sediments. Greigite is common in both strong and weak summer monsoon intervals under 420 m in Heqing core. In greigite bearing sediments, magnetic parameters like magnetic susceptibility and coercivity is dominated by greigite concentration. Greigite prefers to be abundant in terrigenous-rich and organic-poor layers deposited in weak summer monsoon period. Multiple magnetic analysis, particularly discrimination and concentration estimate of greigite, is useful for paleoenvironmental and paleoclimatic reconstructions.

Acknowledgments

We are very grateful to Professor Andrew Roberts for his valuable suggestions which greatly improved the manuscript. This study was supported by the National Science Fund of China (grants 41402151, 41572164), the Key Programs of Frontier Sciences, Chinese Academy of Sciences (grants QYZDY-SSW-DQC001 and ZDBS-SSW-DQC01ZDBS-SSW-DQC01), the Open Fund of the State Key Laboratory of Loess and Quaternary Geology (grant SKLLQG1218), and the Shaanxi Provincial Innovation Team (grant 2014KCT-27). We thank Jan Bloemendal for improving the English.

References

An, Z.S., Clemens, S.C., Shen, J., Qiang, X.K., Jin, Z.D., Sun, Y.B., Prell, W.L., Luo, J.J., Wang, S.M., Xu, H., Cai, Y.J., Zhou, W.J., Liu, X.D., Liu, W.G., Shi, Z.G., Yan, L.B., Xiao, X.Y., Chang, H., Wu, F., Ai, L., Lu, F.Y., 2011. Glacial-interglacial Indian summer monsoon dynamics. Science 333, 719–723.

Ao, H., Deng, C.L., Dekkers, M.J., Liu, Q.S., 2010. Magnetic mineral dissolution in Pleistocene fluvio-lacustrine sediments, Nihewan Basin (North China). Earth Planet. Sci. Lett. 292, 191–200.

Babinszki, E., Márton, E., Márton, P., Kiss, L.F., 2007. Widespread occurrence of greigite in the sediments of Lake Pannon: implications for environment and magnetostratigraphy. Palaeogeography, Palaeoclimatology, Palaeoecology 252, 626–636.

Berner, R.A., 1984. Sedimentary pyrite formation: an update. Geochim. Cosmochim. Acta 48, 605–615.

Blanchet, C.L., Thouveny, N., Vidal, L., 2009. Formation and preservation of greigite (Fe_3S_4) in sediments from the Santa Barbara Basin: implications for paleoenvironmental changes during the past 35 ka. Paleoceanography 24, PA2224. http://dx.doi.org/10.1029/2008PA001719.

Bol'shakov, V.A., Dolotov, A.V., 2011. The curie temperature of the natural greigite (a new interpretation of the thermomagnetic data). Doklady Earth Sci. 440, 1431–1434.

Chang, L., Roberts, A.P., Tang, Y., Rainford, B.D., Muxworthy, A.R., Chen, Q., 2008. Fundamental magnetic parameters from pure synthetic greigite (Fe_3S_4). J. Geophys. Res. 113, B06104. http://dx.doi.org/10.1029/2007JB005502.

Chang, L., Vasiliev, I., Baak, C., Krijgsman, W., Dekkers, M.J., Roberts, A.P., Fitz Gerald, J.D., Hoesel, A., Winklhofer, M., 2014. Identification and environmental interpretation of diagenetic and biogenic greigite in sediments: a lesson from the Messinian Black Sea. Geochem., Geophys., Geosyst. 15. http://dx.doi.org/10.1002/2014GC005411.

Day, R., Fuller, M., Schmidt, V.A., 1977. Hysteresis properties of titanomagnetites: grain size and composition dependence. Phys. Earth Planet. Inter. 13, 260–267.

Dearing, J.A., Battarbee, R.W., Dikau, R., Larocque, I., Oldfield, F., 2006. Human-environment interactions: learning from the past. Reg. Environ. Change 6, 1–16.

Dekkers, M.J., Passier, H.F., Schoonen, M.A.A., 2000. Magnetic properties of hydrothermally synthesized greigite-II. High- and low-temperature characteristics. Geophys. J. Int. 141, 809–819.

Demory, F., Oberhänsli, H., Nowaczyk, N.R., Gottschalk, M., Wirth, R., Naumann, R., 2005. Detrital input and early diagenesis in sediments from Lake Baikal revealed by rock magnetism. Global Planet Change 46, 145–166.

Deng, C.L., Zhu, R.X., Verosub, K.L., Singer, M., Vidic, N., 2004. Mineral magnetic properties of loess/paleosol couplets of the central loess plateau of China over the last 1.2 Myr. J. Geophys. Res. 109, B01103. http://dx.doi.org/10.1029/2003JB002532.

Dong, J., Zhang, S., Jiang, G., Li, H., Gao, R., 2013. Greigite from carbonate concretions of the Ediacaran Doushantuo Formation in South China and its environmental implications. Precambr. Res. 225, 77–85.

Dunlop, D.J., 2002. Theory and application of the Day plot (M_{rs}/M_s versus H_{cr}/H_c) 2. Application to data for rocks, sediments, and soils. J. Geophys. Res. 107, 2057. http://dx.doi.org/10.1029/2001JB000487.

Evans, M.E., Heller, F., Bloemendal, J., Thouveny, N., 1997. Natural magnetic archives of past global change. Surv. Geophys. 18, 183–196.

Fagel, N., Thamó-Bózsó, E., Heim, B., 2007. Mineralogical signatures of Lake Baikal sediments: sources of sediment supplies through Late Quaternary. Sed. Geol. 194, 37–59.

Frank, U., Nowaczyk, N.R., Negendank, J.F.W., 2007. Palaeomagnetism of greigite bearing sediments from the Dead Sea, Israel. Geophys. J. Int. 168, 904–920.

Fu, C.F., Bloemendal, J., Qiang, X.K., Hill, M.J., An, Z.S., 2015. Occurrence of greigite in the Pliocene sediments of Lake Qinghai, China, and its paleoenvironmental and paleomagnetic implications. Geochem., Geophys., Geosyst. 16, 1293–1306. http://dx.doi.org/10.1002/2014GC005677.

Hounslow, M.W., Maher, B.A., 1996. Quantitative extraction and analysis of carriers of magnetization in sediments. Geophys. J. Int. 124, 57–74.

Hüsing, S.K., Dekkers, M.J., Franke, C., Krijgsman, W., 2009. The Tortonian reference section at Monte dei Corvi (Italy): evidence for early remanence acquisition in greigite-bearing sediments. Geophys. J. Int. 179, 125–143.

Jiang, W.T., Horng, C.S., Roberts, A.P., Peacor, D.R., 2001. Contradictory magnetic polarities in sediments and variable timing of neoformation of authigenic greigite. Earth Planet. Sci. Lett. 193, 1–12.

Just, J., Nowaczyk, N.R., Sagnotti, L., Francke, A., Vogel, H., Lacey, J.H., Wagner, B., 2016. Environmental control on the occurrence of high-coercivity magnetic minerals and formation of iron sulfides in a 640 ka sediment sequence from Lake Ohrid (Balkans). Biogeosciences 13, 2093–2109.

Kao, S.J., Horng, C.S., Roberts, A.P., Liu, K.K., 2004. Carbon-sulfur-iron relationships in sedimentary rocks from southwestern Taiwan: influence of geochemical environment on greigite and pyrrhotite formation. Chem. Geol. 203, 153–168.

Kars, M., Kodama, K., 2015. Authigenesis of magnetic minerals in gas hydrate-bearing sediments in the Nankai Trough, offshore Japan. Geochem., Geophys., Geosyst. 16, 947–961. http://dx.doi.org/10.1002/2014GC005614.

Liu, Q.S., Roberts, A.P., Larrasoaña, J.C., Banerjee, S.K., Guyodo, Y., Tauxe, L., Oldfield, F., 2012. Rock and environmental magnetism: principles and applications. Rev. Geophys. 50, RG4002. http://dx.doi.org/10.1029/2012RG000393.

Minyuk, P.S., Tyukova, E.E., Subbotnikova, T.V., Kazansky, A.Y., Fedotov, A.P., 2013. Thermal magnetic susceptibility data on natural iron sulfides of northeastern Russia. Russ. Geol. Geophys. 54, 464–474.

Murdock, K.J., Wilkie, K., Brown, L.L., 2013. Rock magnetic properties, magnetic susceptibility, and organic geochemistry comparison in core LZ1029-7 Lake El'gygytgyn, Russia Far East. Climate of the Past Discussions 9, 467–479.

Muxworthy, A.R., Dunlop, D.J., 2002. First-order reversal curve (FORC) diagrams for pseudo-single-domain magnetites at high temperature. Earth Planet. Sci. Lett. 203, 369–382.

Nolan, S.R., Bloemendal, J., Boyle, J.F., Jones, R.T., Oldfield, F., Whitney, M., 1999. Mineral magnetic and geochemical records of late Glacial climatic change from two northwest European carbonate lakes. J. Paleolimnol. 22, 97–107.

Oldfield, F., Maher, B.A., Donoghue, J., Pierce, J.W., 1985. Particle-size related, mineral magnetic source sediment linkages in the Rhode River catchment, Maryland, USA. J. Geol. Soc. London 142, 1035–1046.

Oldfield, F., 2013. Mud and magnetism: records of late Pleistocene and Holocene

environmental change recorded by magnetic measurements. J. Paleolimnol. 49, 465–480.
Passier, H.F., de Lange, G.J., Dekkers, M.J., 2001. Magnetic properties and geochemistry of the active oxidation front and the youngest sapropel in the eastern Mediterranean Sea. Geophys. J. Int. 145, 604–614.
Pike, C.R., Roberts, A.P., Verosub, K.L., 1999. Characterizing interactions in fine magnetic particle systems using first order reversal curves. J. Appl. Phys. 85, 6660–6667.
Porreca, M., Mattei, M., DiVincenzo, G., 2009. Post-deformational growth of late diagenetic greigite in lacustrine sediments from southern Italy. Geophys. Res. Lett. 36, L09307. http://dx.doi.org/10.1029/2009GL037350.
Reinholdsson, M., Snowball, I., Zillén, L., Lenz, C., Conley, D.J., 2013. Magnetic enhancement of Baltic Sea sapropels by greigite magnetofossils. Earth Planet. Sci. Lett. 366, 137–150.
Reynolds, R.L., Rosenbaum, J.G., van Metre, P., Tuttle, M., Callender, E., Goldin, A., 1999. Greigite (Fe_3S_4) as an indicator of drought-The 1912–1994 sediment magnetic record from White Rock Lake, Dallas, Texas, USA. J. Paleolimnol. 21, 193–206.
Roberts, A.P., 1995. Magnetic properties of sedimentary greigite (Fe_3S_4). Earth Planet. Sci. Lett. 134, 227–236.
Roberts, A.P., Reynolds, R.L., Verosub, K.L., Adam, D.P., 1996. Environmental magnetic implications of greigite (Fe_3S_4) formation in a 3 million year lake sediment record from Butte Valley, Northern California. Geophys. Res. Lett. 23, 2859–2862.
Roberts, A.P., Pike, C.R., Verosub, K.L., 2000. First-order reversal curve diagrams: a new tool for characterizing the magnetic properties of natural samples. J. Geophys. Res. 105, 28461–28475.
Roberts, A.P., Weaver, R., 2005. Multiple mechanisms of remagnetization involving sedimentary greigite (Fe_3S_4). Earth Planet. Sci. Lett. 231, 263–277.
Roberts, A.P., Liu, Q., Rowan, C.J., Chang, L., Carvallo, C., Torrent, J., Horng, C.S., 2006. Characterization of hematite (α-Fe_2O_3), goethite (α-FeOOH), greigite (Fe_3S_4), and pyrrhotite (Fe_7S_8) using first-order reversal curve diagrams. J. Geophys. Res. 111, B12S35. http://dx.doi.org/10.1029/2006JB004715.
Roberts, A.P., Chang, L., Rowan, C.J., Horng, C.-S., Florindo, F., 2011. Magnetic properties of sedimentary greigite (Fe_3S_4): an update. Rev. Geophys. 49, RG1002. http://dx.doi.org/10.1029/2010RG000336.
Roberts, A.P., Heslop, D., Zhao, X., Pike, C.R., 2014. Understanding fine magnetic particle systems through use of first-order reversal curve diagrams. Rev. Geophys. 52, 557–602.
Roberts, A.P., 2015. Magnetic mineral diagenesis. Earth Sci. Rev. 151, 1–47.
Robinson, S.G., Sahota, J.T.S., 2000. Rock-magnetic characterization of early, redoxomorphic diagenesis in turbiditic sediments from the Madeira Abyssal Plain. Sedimentology 47, 367–394.
Ron, H., Nowaczyk, N.R., Frank, U., Schwab, M.J., Naumann, R., Striewski, B., Agnon, A., 2007. Greigite detected as dominating remanence carrier in Late Pleistocene sediments, Lisan formation, from Lake Kinneret (Sea of Galilee), Israel. Geophys. J. Int. 170, 117–131.
Rowan, C.J., Roberts, A.P., 2006. Magnetite dissolution, diachronous greigite formation, and magnetizations arising from pyrite oxidation: unravelling complex magnetizations in Neogene marine sediments from New Zealand. Earth Planet. Sci. Lett. 241, 119–137.
Rowan, C.J., Roberts, A.P., Broadbent, T., 2009. Reductive diagenesis, magnetite dissolution, greigite growth and paleomagnetic smoothing in marine sediments: a new view. Earth Planet. Sci. Lett. 277, 223–235.
Skinner, B.J., Grimaldi, F.S., Erd, R.C., 1964. Greigite, the thio-spinel of iron: a new mineral. Am. Mineral. 49, 543–555.
Snowball, I., Thompson, R., 1988. The occurrence of greigite in sediments from Loch Lomond. J. Quat. Sci. 3, 121–125.
Sagnotti, L., Winkler, A., 1999. Rock magnetism and palaeomagnetism of greigite-bearing mudstones in the Italian peninsula. Earth Planet. Sci. Lett. 165, 67–80.
Su, Y.L., Gao, X., Liu, Q.S., Wang, J.B., Haberzettl, T., Zhu, L.P., Li, J.H., Duan, Z.Q., Tian, L.D., 2013. Mineral magnetic study of lacustrine sediments from Lake Pumoyum Co, southern Tibet, over the last 19 ka and paleoenvironmental significance. Tectonophysics 588, 209–221.
Thompson, R., Morton, D.J., 1979. Magnetic susceptibility and particle size distribution in recent sediments of the Loch Lomond drainage basin, Scotland. J. Sediment. Res. 49, 801–811.
Torii, M., Fukuma, K., Horng, C.S., Lee, T.Q., 1996. Magnetic discrimination of pyrrhotite- and greigite-bearing sediment samples. Geophys. Res. Lett. 23, 1813–1816.
Tric, E., Laj, C., Jehanno, C., Valet, J.P., Kissel, C., Mazaud, A., Iaccarino, S., 1991. High-resolution record of the Upper Olduvai transition from Po Valley (Italy) sediments: support for dipolar transition geometry? Phys. Earth Planet. Inter. 65, 319–336.
Verosub, K.L., Roberts, A.P., 1995. Environmental magnetism: past, present, and future. J. Geophys. Res. 100, 2175–2192.
Xiao, X.Y., Shen, J., Wang, S.M., Xiao, H.F., Tong, G.B., 2010. The variation of the southwest monsoon from the high resolution pollen record in Heqing Basin, Yunnan Province, China for the last 2.78 Ma. Palaeogeography, Palaeoclimatology, Palaeoecology 287, 45–57.